

Programmable photonics for free space optics communications and computing

A. Melloni^{*1}, A. Martinez¹, G. Cavicchioli¹, S. Seyedinnavadeh¹,
F. Zanetto¹, D.A.B. Miller² and F. Morichetti¹

1. DEIB, Politecnico di Milano, via Ponzio 34/5, 20133, Milan, Italy
2. Ginzton Laboratory, Stanford University, Spilker Building, Stanford, CA, 94305, USA
**andrea.melloni@polimi.it*

Abstract — Establish multiple and robust communication channels through arbitrary complex optical media is demonstrated by using integrated photonic processors based on meshes of Mach-Zehnder interferometers. The receiver is capable of compensating for scintillation induced by atmospheric turbulence automatically, without any need of knowledge of the link. The processor is able to perform a physical Singular Value Decomposition operation and any other algebraic operation.

Keywords— Free space optics, programmable photonics, optical processor, optical computing, silicon photonics

I. INTRODUCTION

In Free Space Optics (FSO) communication systems, atmospheric turbulence introduces a random phase and amplitude perturbation to the propagating optical beams [1]. This effect is known as scintillation and causes a deep fading of the signal at the photodetector. These perturbations can be compensated using a multi-aperture receiver that samples the distorted wavefront on different points and adds the different contributions coherently [2].

In this paper, we report an adaptive optical receiver that consists of an optical phased array (OPA) and a programmable optical processor (POP). A self-adaptive control scheme enables an automatic handling of the scintillation without any need of knowledge of the media itself and without the pre-calibration of the mesh elements. Experimental results demonstrate the effectiveness of the approach with intensity modulated optical signals at a data rate of 10 Gbit/s.

II. INTEGRATED FSO PHOTONIC RECEIVER

The integrated FSO photonic receiver (IFPRx) has been designed to compensate for turbulence with a scintillation index up to $\sigma_I^2 = 10^{-2}$, corresponding to a realistic link of several

hundreds of meters. A schematic of the receiver is shown in Fig. 1(a). An array of 16 surface grating couplers (GCs), distributed in two concentric rings, compose the 2D optical phased array (OPA). The distance between the GCs has been optimized to match the coherence radius r_0 (Fried parameter) of the beam in the maximum turbulence conditions.

The programmable optical processor (POP) is a 16×1 binary-tree mesh of thermally tunable Mach-Zehnder Interferometers (MZIs). Each MZI is dithered independently [3] using two thermal phase-shifters (heaters) integrated on top of the inner and outer waveguides of the MZI. Integrated Ge photodetectors (PD) are used to control the state of each MZI in order to coherently combine the input signals maximizing the output power [4,5]. The IFPRx, is realized on a standard 220-nm silicon photonic platform (AMF foundry) and is designed to work in the C-band (Fig. 1b).

This architecture of the receiver allows to control independently each GC and hence the shape of the radiated beam. For instance, Fig. 1(c₁) depicts a photograph of the light emitted by the OPA in its native state, whereas in Fig. 1(c₂) the heaters were driven to distribute the light approximately equally among all the GCs.

III. EXPERIMENTAL RESULTS

To validate the IFPRx we built a 3-m-long indoor FSO link emulator that generate a beam with a diameter around 5 cm and could vary the turbulence strength from an effective refractive index parameter $C_n^2 = 10^{-14}$ to 10^{-10} [$\text{m}^{-2/3}$]. Fig. 2(a₁) shows a photo of the received beam in absence of turbulence and Fig. 2(a₂) the received turbulent beam. To couple the received beam with the OPA, we employed a biconcave lens and a dielectric mirror (Fig. 2b). Due to the size of the beam and short length of the link, the wander effect was negligible.

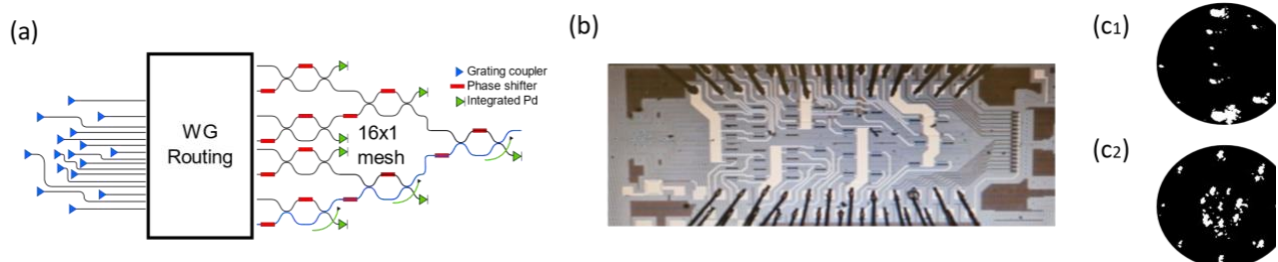


Fig. 1: (a) schematic of the integrated photonic receiver, (b) an image of the realized device in silicon photonic platform, (c₁) native state of the IFPRx with all the MZIs in cross state and (c₂) with the POP is reconfigured to emit the same power from each grating.

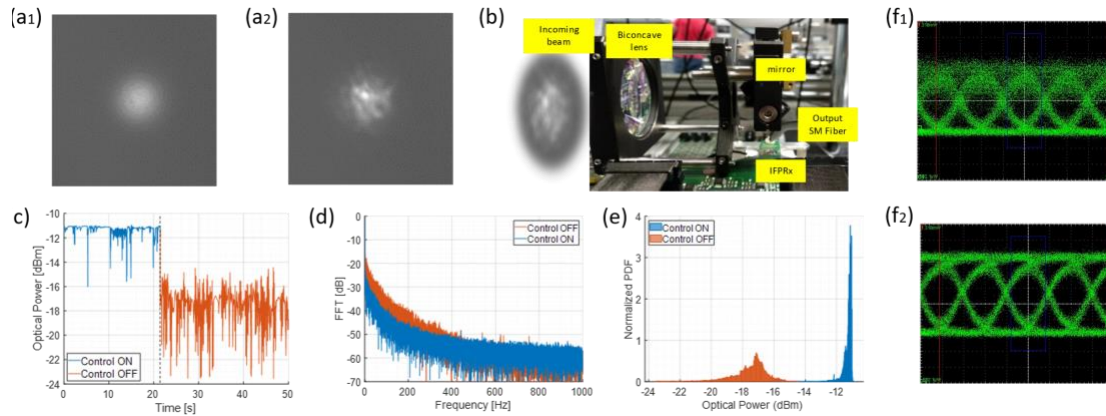


Fig. 2: Gaussian beam generated indoors (a₁) without turbulence and (a₂) with artificial turbulence. (b) Photo of the experimental setup. (c) Optical power, (d) power spectral density, and (e) probability density function of the received optical signal when the control is ON (blue) and OFF (orange). Eye diagrams when control is (f₁) ON and (f₂) OFF.

Fig. 2c shows the received optical power when the adaptive control is OFF (orange) and ON (blue). When the control is ON, the IFPRx compensates for the relative phase differences between the signals maximizing the output power. The average received power at the output port of the IFPRx is -11.3 dBm with a standard deviation of 0.3 dB. Due to the “speckles” of the turbulent beam, there are cases for which some GCs may receive less power causing a small fading in the received power. On the other hand, when the control is OFF, the random phase front of the incoming scintillated beam determines whether the 16 acquired signals interact constructively or destructively. For this reason, the received power presents a larger standard deviation ($\text{std} = 1.2$ dB) and a lower mean (-17.6 dBm).

The spectral power density of the received signal is shown in Fig. 2(d). The components associated with the turbulence (orange) extend up to a frequency range of about 500 Hz. The IFPRx was able to reduce these components by more than 7 dB up to 400 Hz (blue), which is sufficient to compensate natural turbulence (300 Hz) [6]. Despite the many decays of the received power with the control ON (Fig. 2c), the probability density function (PDF) (Fig. 2e) shows a narrow distribution with most of the power concentrated within -11.5 and -11 dBm (with a small peak at -12.2 dBm). Instead, when the control is OFF the PDF has its maximum around -17 dBm and spreads through several dB (from -24 to -14.5 dBm).

System-level measurements were performed using an OOK NRZ modulated 10 Gbps signal. Fig. 2(f₁) shows the received eye diagram when the adaptive control is OFF. It is evident that the amplitude variations caused by scintillation introduce noise to the eye diagram. Instead, when the control loop is active (Fig. 2f₂), the eye remains open, proving the effective mitigation of scintillation effects.

By using a photonic processor also at the transmitter, multiple channels can be handled. The system performs generation, manipulation, and shaping of the optical beams, and is able to establish automatically orthogonal free-space channels through scattering media. The self-configuration process consists of injecting the light iteratively back and forward into the WGs of the Tx and Rx processor and minimizing the lower output port of each MZI in each row, without needing any calibration or calculations [6,7].

IV. CONCLUSION

In conclusion, we demonstrated the effectiveness of an integrated adaptive receiver based on a 2D optical phase array and programmable photonic processor to compensate the scintillation effects in a turbulent FSO link. Results show an effective reduction of intensity fading for turbulent conditions stronger than those expected in a natural environment. The performance of the receiver can be improved by increasing the number of optical antennas to compensate for the intensity fading. Also, by increasing the bandwidth of the control loop, the high frequency components could be further attenuated.

ACKNOWLEDGMENT

The research has been carried out in the framework of the Huawei-Politecnico di Milano Joint Research Lab and the Italian National Recovery and Resilience Plan (NRRP) of NextGenerationEU, partnership on “Telecommunications of the Future” (PE00000001 - program “RESTART”, Structural Project “Rigoletto” and Focused Project “HePIC”). Part of this work was carried out at Polifab, Politecnico di Milano, Milan, Italy (www.polifab.polimi.it).

REFERENCES

- [1] X. Zhu and J. M. Kahn, "Free-space optical communication through atmospheric turbulence channels," *IEEE Transactions on Communications*, 50, 8, 1293-1300, 2002.
- [2] M.A. Cox et al, "Structured Light in Turbulence", *IEEE JSTQE*, 27, 2, 2021
- [3] F. Zanetto, V. Grimaldi, F. Toso et al, "Dithering-based real-time control of cascaded silicon photonic devices by means of non-invasive detectors," in *IET Optoelectron*, 15: 111-120, 2021.
- [4] M. Milanizadeh, S. SeyedinNavadeh, et al, Separating arbitrary free-space beams with an integrated photonic processor. *Light Sci. Appl.* 11, 2022
- [5] Y. Wang, H. Xu, D. Li et al. "Performance analysis of an adaptive optics system for free-space optics communication through atmospheric turbulence," in *Scientific Report* 8, pp. 1124. 2018.
- [6] S. Pai et al., Experimentally realized in situ backpropagation for deep learning in photonic neural networks, *Science*, 27 Apr 2023, 380, 6643
- [7] D.A.B. Miller, "Establishing Optimal Wave Communication Channels Automatically," in *Journal of Lightwave Technology*, 31, 24, 3987-3994, Dec. 2013, doi: 10.1109/JLT.2013.2278809